

Dynamic Analysis of Pneumatically Actuated Mechanisms

Arturo Lara-López, Joaquín Pérez-Meneses, José Colín-Venegas*,

Eduardo Aguilera-Gómez and Jesús Cervantes-Sánchez

Mechanical Engineering Department, University of Guanajuato at Salamanca

Palo Blanco, Salamanca, Gto., México

Phone: +52 (464) 647-9940, Fax: +52 (464) 647-9940 ext. 2311

*Corresponding author email: colin@salamanca.ugto.mx

Resumen

En este artículo se analiza el comportamiento dinámico de sistemas impulsados neumáticamente. Primeramente se analiza un modelo básico que consiste de un eslabón montado sobre un eje impulsado neumáticamente contra una fuerza externa. El modelo matemático que resulta es el fundamento básico para formular modelos de mecanismos más complejos. Luego, el análisis se extiende a un mecanismo de cuatro barras donde el eslabón de entrada se impulsa por un cilindro neumático y la fuerza externa es aplicada contra el eslabón de salida. Los modelos para ambos sistemas se obtuvieron de la aplicación directa de principios dinámicos y termodinámicos y de relaciones de la cinemática, incorporando características físicas de los mecanismos y el efecto de condiciones del aire, tamaño del tanque y amortiguamiento del pistón. Tales parámetros pueden manipularse con propósitos de diseño. Se construyeron prototipos experimentales de ambos modelos (un eslabón montado sobre un eje y un mecanismo de cuatro barras) para medir su respuesta dinámica. Los datos experimentales se compararon con la solución teórica mostrando buena similitud.

Abstract

The dynamic behavior of pneumatically driven systems is analyzed in this paper. First a basic model consisting of a single pivoted link pneumatically actuated against an external force is discussed. Resulting mathematical model is the basic foundation to formulate models for more complex mechanisms. Then, the analysis is extended to a four bar mechanism, where the input link is driven by a pneumatic cylinder and the external force is applied against the output link. Models for both systems were obtained from direct application of dynamic and thermodynamic principles and kinematics relations, incorporating physical characteristics of the mechanisms and the effect of air conditions, tank size and piston cushion. Such parameters can be manipulated for design purposes. Experimental apparatus were constructed to measure the dynamic response of both models (the single pivoted link and the four bar mechanism). Experimental data where compared with the theoretical response showing good agreement.

Palabras clave:

Mecanismos impulsados neumáticamente, dinámica de mecanismos

Introduction

It is a well recognized fact that increasing productivity in the high technology systems demanded by today's industry largely relies upon the ability of machines in service to run at higher speeds while still maintaining the desired dynamic behavior and precision. Many of these machines include pneumatically driven pivoted links or mechanism. Then the knowledge of the transient response of high speed linkages may be of great interest for industry to meet the compromise between speed of process and avoidance of damage to products, especially when excessive acceleration may damage products being handled. This naturally poses a challenge to machine design engineers for reliable and precise prediction of consequences resulting from an increment of the operation speed. In addition, one more difficulty is due to the inability of commercial computer-based design tools to include realistic properties in models of the dynamic behavior of pneumatic systems. Practical modeling techniques also need to be computationally efficient and should be experimentally verified, hence the motivation to write this paper.

Key words:

Pneumatically actuated mechanisms, dynamics of mechanisms

The models presented in this article include important machine dynamic properties, such as those related to the compressed air in a tank, a pneumatic actuator with an exhaust valve that permits to regulate the start and end cushion periods and the kinematics and dynamics properties of the impulse link or mechanism, that could be under the action of external forces including dry and viscous friction and the useful force. It is expected that the contribution of this article would be centered in a new model that integrates as completely as possible the performance of the whole system, this means the pneumatic circuit with the kinematics and dynamics of the mechanism and the analysis of the influence of their parameters. In addition the resulting model is simpler than those related to similar problems previously published with no additional simplifying hypothesis. Moreover, the theoretical response of the whole system was experimentally verified.

A number of important contributions oriented to understand and predict the dynamic performance of this type of pneumatically driven devices are in the literature. A summary is presented.

Bobrow and Jabbari (1991) modeled this type of mechanism considering the rigid body equation of motion for pivoted link in addition to the energy equation for the air in the cylinder. Pressure in the inlet of the cylinder was assumed as constant. Authors emphasize the nonlinear characteristic of the system. J. Tang and G. Walker (1995) proposed a model to simulate the movement of a pneumatic actuator based on the equation of motion of a translating mass under friction force which includes dry and viscous components. That paper presents the control analysis of the system. M. Skreiner and P. Barkan (1971) proposed a model for a four bar linkage driven by a pneumatic actuator. This model was analyzed as a control system based on two equations. The first one is a kinematic equation and the second one is the control equation. Kiczkowiak (1995) proposed a model to simulate the dynamic performance of a cylinder driving links of a manufacturing machine tool. Kawakami et al (1988) proposed a model for pneumatic cylinder considering the dynamics of the piston and thermodynamics of the air. Such model shows that the heat transfer from the cylinder has little effect on movement of the piston. Authors emphasized the nonlinear characteristic of the cylinder. Aguilera and Lara (1999) proposed a model to predict the dynamic performance of a cylinder actuating on a translating mass under resistive forces taking into consideration the dimensions of the system, and basing its formulation on dynamic and thermodynamic considerations. Start and end cushion periods are considered in the modeling.

The Basic Model: a Pivoted Link.

As mentioned before, the basic model includes a pivoted link driven by a pneumatic system, as shown schematically in Fig. 1. In the following subsections the analysis involved in the development of the whole theoretical model, is presented.

Joint kinematics

Figure 1 shows the schematic configuration of the actuated linkage, which can be completely described by means of the vector of joint variables $q \equiv (r; \phi, \theta_2)^T$. These selected joint variables are related by a set of constraint equations that come from the vector loop-closure that is detected for the linkage. Similarly the joint velocity vector $\dot{q} \equiv (\dot{r}; \dot{\phi}, \dot{\theta}_2)^T$ and the joint acceleration vector $\ddot{q} \equiv (\ddot{r}; \ddot{\phi}, \ddot{\theta}_2)^T$ are defined as function of the time derivatives of the joint variables. Thus, the vector-loop closure gives:

$$r e^{j\phi} - p e^{j\theta_2} - L e^{j0} = 0 \quad (1)$$

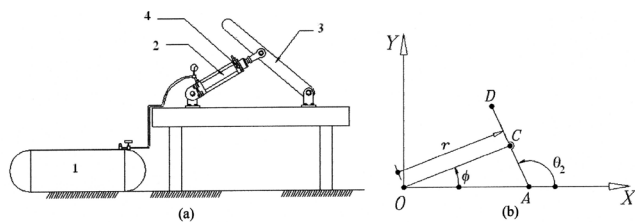


Figure 1. Basic Model, (a) Schematic diagram, including a pivoted link (3) driven by a pneumatic actuator (2) with exhaust control valve (4) and tank (1), (b) Kinematic layout of the actuated pivoted link.

where $L \equiv OA$ and $p \equiv AC$.

Then, given the input motion r, \dot{r} and \ddot{r} a closed-form solution for the remaining joint variables and their time derivatives may be obtained, namely: (Shigley & Uicker, 1995)

$$\phi = 2 \arctan \left(\pm \sqrt{\frac{2rL + A}{2rL - A}} \right) \quad (2)$$

$$\theta_2 = 2 \arctan \left(\pm \sqrt{\frac{2Lp + B}{2Lp - B}} \right) \quad (3)$$

$$\dot{\phi} = \frac{\dot{r}(L \cos \phi - r)}{L r \sin \phi} \quad (4)$$

$$\dot{\theta}_2 = \frac{\dot{r} \sin \phi + r \dot{\phi} \cos \phi}{p \cos \theta_2} \quad (5)$$

$$\ddot{\phi} = \frac{\ddot{r}(L \cos \phi - r) - \dot{r}(\dot{r} + 2L\dot{\phi} \sin \phi) - Lr\dot{\phi}^2 \cos \phi}{L r \sin \phi} \quad (6)$$

$$\ddot{\theta}_2 = \frac{-(\ddot{r} - r\dot{\phi}^2) \cos \phi + (2\dot{r}\dot{\phi} + r\ddot{\phi}) \sin \phi - \dot{\theta}_2^2 p \cos \theta_2}{p \sin \phi} \quad (7)$$

Where the involved geometric parameters (see Fig. 1) are defined as follows:

$$A \equiv p^2 - r^2, \quad B \equiv p^2 + L^2 - r^2.$$

Dynamic Analysis

Forces acting on the piston and rod are shown in Fig. 2a. It is assumed that the weight and the moment of inertia corresponding to the piston and rod are small, causing negligible normal forces N_p and N_o . The main reason for this assumption comes from the idea that the useful axial force on the rod F should be much greater than the weight of the cylinder.

Applying Newton's Second Law to the pivoted link (Fig. 2b and Fig. 2c), in order to find an expression for the piston force F , the resulting equations are:

$$A_x + F_x = m_b a_x \quad (8)$$

$$A_y + F_y - W_b = m_b a_y \quad (9)$$

$$M_F - M_W = I_A \ddot{\theta}_2 \quad (10)$$

where A_x, A_y are the components of the reaction force acting on the pivoted link at point A , F_x, F_y are the components of the reaction force between piston and link, m_b is the mass of the link, a_x, a_y are the components of the acceleration of the center of gravity of the link, M_F and M_W are the moments due to the useful force, F , and weight of link, W_b , about A respectively,

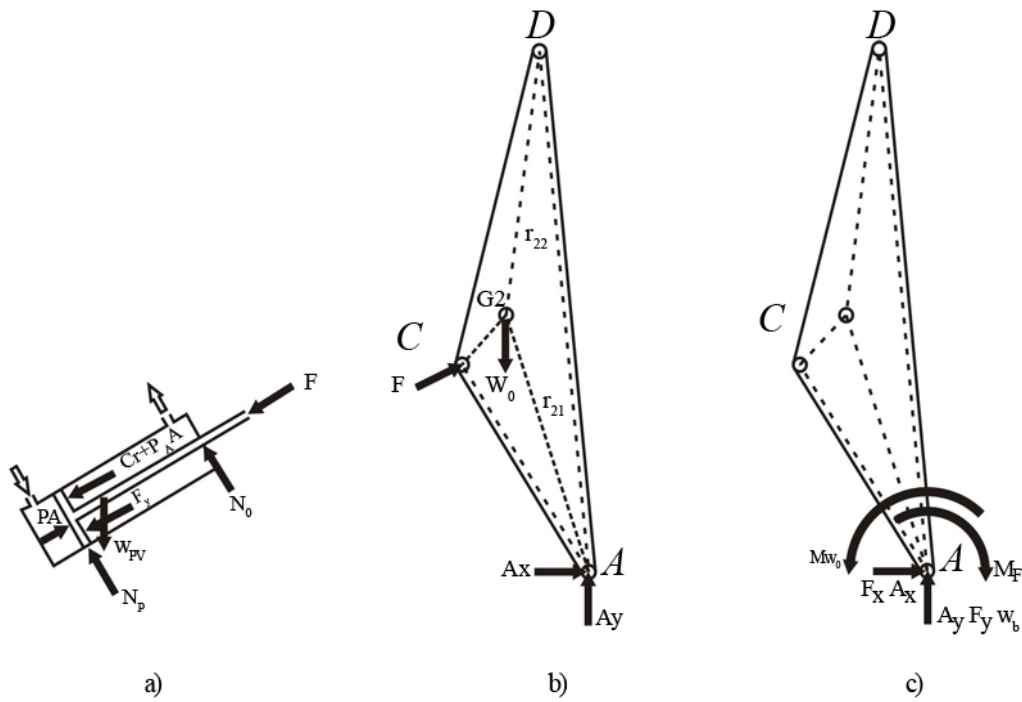


Figure 2. a) Free body diagram of Piston and rod, b) Free body diagram of the Pivoted link, and c) Modified free body diagram with forces translated to the pivoted axle and resulting moments.

and are given by $M_F = F_p \sin(\phi + \theta_2)$, $M_{W_b} = r_{21} W_b \cos \theta_2$, and I_A is the moment of inertia of the link about point A which is defined as $I_A = \frac{1}{3} m_b d^2$ for a rectangular bar (as in the experimental apparatus), with a length d .

Substituting the above into equation (10) and simplifying, the following equation for the force F acting on piston is obtained:

$$F = \frac{m_b d^2}{3L^2 \sin^2 \phi} (\ddot{r} - \dot{r} \dot{\phi} \cot \phi) + \frac{W_b r_{21} (L - r \cos \phi)}{pL \sin \phi} \quad (11)$$

Thermodynamic Analysis.

In order to incorporate the influence of the air properties into the whole model, the following assumptions will be considered:

- a) The volume of the air in the tank remains constant, b) the pressure and temperature of the air in the tank are known before expansion, c) the air behaves as an ideal gas, d) waves of pressure and temperature are neglected, e) forces against the piston include dry and viscous friction, atmospheric pressure and force on the rod, f) friction on mechanism joints is negligible, g) changes of kinetic and potential energy of the air in the system will be neglected, and h) air leakage from cylinder is negligible.

The First Law of thermodynamics states that the energy entering to the control volume of a system as heat or mechanical work is transformed into a change of energy of the air contained in such control volume. For an open system and considering the space in the high pressure side of the piston as the control volume, the following equation may be written:

$$u_2 m_2 - u_1 m_1 = h_o m_{in} + Q - W_{air} \quad (12)$$

where Q is the heat transfer between the control volume and its boundary occurring during the process from an initial state (1) and any other state (2), W_{air} is the work done on the air contained in the control volume between the initial state 1 and a second state 2, u_1 and u_2 are the internal energy of air per unit of mass corresponding to states 1 and 2 respectively, h_o is the initial enthalpy of air per unit of mass, m_1 and m_2 are the mass of air in the control volume for initial state and a second state respectively, and m_{in} is the increment of mass in the control volume between states 1 and 2.

The principle of conservation of mass related to the control volume may be written as:

$$m_2 - m_1 = m_{in} \quad (13)$$

Substituting m_{in} from equation (13) into equation (12):

$$(u_2 - h_o)m_2 = (u_1 - h_o)m_1 + Q - W_{air} \quad (14)$$

For ideal gases the following well known equations apply:

$$m = \frac{PV}{RT} \quad (15)$$

$$du = C_v dT \quad (16)$$

$$h = u + RT \quad (17)$$

$$C_p - C_v = R \quad (18)$$

where P , V , T , u and h are, respectively, the pressure, volume, absolute temperature, internal energy and enthalpy of the gas in the system. Moreover, C_p and C_v are specific heat of the air and R the universal constant for ideal gases.

Substituting R from equation (18) into equation (17) and referring the resulting equation to the initial and a second state:

$$(u_1 - h_0) = C_v T_1 - C_p T_0 \quad (19)$$

$$(u_2 - h_0) = C_v T_2 - C_p T_0 \quad (20)$$

Substituting equations (19) and (20) into equation (14) it follows:

$$(C_v T_2 - C_p T_0) m_2 = m_1 (C_v T_1 - C_p T_0) + Q - W_{air} \quad (21)$$

Based on the mechanical hypothesis mentioned above, the work done by the weight of piston and rod and the normal forces on these elements is not considered, being the work on the piston and rod as follows:

$$W = W_{air} - \int P_A A_A dr - \int C \dot{r} dr - F_F (r - r_0) - \int F dr \quad (22)$$

when $|\dot{r}| > 0$

where W_{air} is the work done by the air on the high pressure side of the piston, C is the constant coefficient for viscous friction, F_F is the dry friction force against the movement of the piston, F is the force on the piston rod, P_A is the atmospheric pressure and A_A is the piston area on the rod side.

Assuming that the process starts from the static equilibrium, then, the principle of work and kinetic energy applied to the piston and rod may be expressed as follows:

$$W = \frac{1}{2} m_p (\dot{r}^2 + r^2 \dot{\phi}^2) \quad (23)$$

where m_p is the combined mass for the piston and rod.

Substituting equation (23) into equation (22) the following equation is obtained:

$$\begin{aligned} W_{air} - \int P_A A_A dr - \int C \dot{r} dr - F_F (r - r_0) - \int F dr = \\ = \frac{1}{2} m_p (\dot{r}^2 + r^2 \dot{\phi}^2) \end{aligned} \quad (24)$$

Now, substituting W_{air} from equation (24) into equation (21), follows that:

$$\begin{aligned} (C_v T_2 - C_p T_0) m_2 = m_1 (C_v T_1 - C_p T_0) - \frac{1}{2} m_p (\dot{r}^2 + r^2 \dot{\phi}^2) - \\ - \int P_A A_A dr - \int C \dot{r} dr - F_F (r - r_0) - \int F dr + Q \end{aligned} \quad (25)$$

Now, applying Newton's Second Law to the piston (see Fig. 2a), the following equation results:

$$P_A - P_A A_A - F_F - F - C \dot{r} = m_p (\ddot{r} - r \dot{\phi}^2) \quad (26)$$

when $|\dot{r}| > 0$

where A is the piston area on the high pressure side.

Combining equations (15) and (26) for the specific conditions of a second state, for any position of the piston, the absolute temperature for this state may be expressed as:

$$T_2 = \left(\frac{V_0 + A(r - r_0)}{m_2 R} \right) \left(\frac{m_p (\ddot{r} - r \dot{\phi}^2) + P_A A_A + F_F + F + C \dot{r}}{A} \right) \quad (27)$$

Where m_2 is the mass of air in the control volume for such a second state, $r - r_0$ is the displacement of the piston from the initial position to that corresponding to the second state. Substituting equations (27) and (11) into equation (25) and simplifying, the following equation may be written:

$$\begin{aligned} & \left\{ \frac{2C_v (V_0 + A(r - r_0))}{AR} + \left[\frac{2C_v}{m_p} \left(\frac{V_0 + A(r - r_0)}{AR} \right) + \frac{2r}{m_p} \right] \left[\frac{W_b p^2}{3g \sin \phi (L \cos \phi - r)} \right] \right\} \dot{r} + \\ & + r \dot{\phi}^2 \left[\frac{2C_v (V_0 + A(r - r_0))}{AR} - r \right] + \dot{r} \left[\dot{r} + \frac{2C_v (V_0 + A(r - r_0)) C}{m_p A R} \right] + \\ & + \frac{2C_v}{m_p} \left[\left(\frac{V_0 + A(r - r_0)}{AR} \right) (P_A A_A + F_F) - m_1 T_1 \right] - \frac{2C_p T_0}{m_p} (m_2 - m_1) + \\ & + \left[\frac{2C_v}{m_p} \left(\frac{V_0 + A(r - r_0)}{AR} \right) + \frac{2r}{m_p} \right] \left[\frac{W_b d^2}{3g L^2 \sin^2 \phi} (-\dot{r} \dot{\phi} \cot \phi) + \frac{W_b r_{21} (L - r \cos \phi)}{p L \sin \phi} \right] + \\ & + \frac{2}{m_p} \left[F_F (r - r_0) + \int P_A A_A dr + \int C \dot{r} dr \right] - \frac{2}{m_p} Q = 0 \end{aligned} \quad (28)$$

For completion of the simulation model it is necessary to use equation (29) for nozzle mass flow rate, Anderson B. W. (2001), where the factor K is given by equation (30).

$$\dot{m}_{12} = \frac{K P_1 A_{12} N_{12}}{g \sqrt{T_1}} \quad (29)$$

$$K = \left[\frac{gk}{R} \left(\frac{2}{k+1} \right)^{(k+1)/(k-1)} \right]^{\frac{1}{2}} \quad (30)$$

where R is the universal constant for ideal gases, g is the acceleration of gravity, A_{12} is the section area for flow the air, P_1 and T_1 are the total pressure and temperature in the state 1, that is, at the local isentropic stagnation state. The factor N_{12} is given by

$$N_{12} = \left[\frac{\left(\frac{P_2}{P_1} \right)^{2/k} - \left(\frac{P_2}{P_1} \right)^{(k+1)/k}}{\frac{k-1}{2} \left(\frac{2}{k+1} \right)^{(k+1)/(k-1)}} \right]^{\frac{1}{2}} \quad (31)$$

where P_2 is the pressure and T_2 is the temperature in the second state.

The factor N_{12} is a function of the ratio of specific heats and pressures. Therefore, it is nearly the same for all diatomic gases; in this case k is approximately 1.4. The isentropic process relating P_1 and P_2 determines the relationships between temperature and pressure and between density, ρ , and pressure.

These are:

$$\frac{\rho_2}{\rho_1} = \left(\frac{P_2}{P_1} \right)^{1/k} \quad (32)$$

$$\frac{T_2}{T_1} = \left(\frac{P_2}{P_1} \right)^{(k-1)/k} \quad (33)$$

Simulation Procedure.

Finally, equations (6) and (28) constitute the mathematical model used to predict the dynamic performance of the system. Both equations were solved by Runge Kutta fourth order numerical method. However, those equations constitute a non linear second order system of differential equations where the variables \ddot{r} and $\ddot{\phi}$ were both obtained iteratively as follows; In the first iteration the initial value for the variables r and ϕ , that is r_0 and ϕ_0 were substituted into equation (28) and then using Runge Kutta numerical method that equation was solved for \ddot{r} . The value obtained was introduced in equation (6) in order to solve for $\ddot{\phi}$. The result from the first iteration was used as the initial value for the next iteration, and so on. The displacement of the piston is the variable that stops the iterations when its stroke is completed.

EXTENDED MODEL: FOUR BAR LINKAGE.

Now, the analysis made to the basic model is extended to a four bar linkage, where the input link is driven by a pneumatic system, and the external force is applied to the output link. Figure 3 shows a layout of the complete system. In the following subsections it is presented the analysis involved in the development of the whole theoretical model.

Kinematic analysis

A kinematic layout of the linkage under study is now shown in Fig. 3. In order to develop a systematic procedure, the kinematics analysis of the linkage will be divided in two parts, namely, joint kinematics and point kinematics.

Joint kinematics

As shown in Fig. 3, the configuration of the actuated four bar linkage can be completely described by means of the vector of joint variables $q = (r, \phi, \theta_2, \theta_3, \theta_4)^T$, where r , ϕ and θ_2 are the joint variables defined for the basic model. The remaining joint variables θ_3 and θ_4 are related with θ_2 by a set of constraint equations that come from the vector loop-closure that is detected for the four bar linkage. Thus, referring to Fig. 3, the vector loop-closures give the following equation in addition to equation (1):

$$d e^{j\theta_2} + s e^{j\theta_3} - l e^{j\theta_4} - h e^{j0} = 0 \quad (34)$$

Thus, given the input motion r a closed-form solution for the joint variables may be obtained from the following equations in addition to equations (2) and (3):

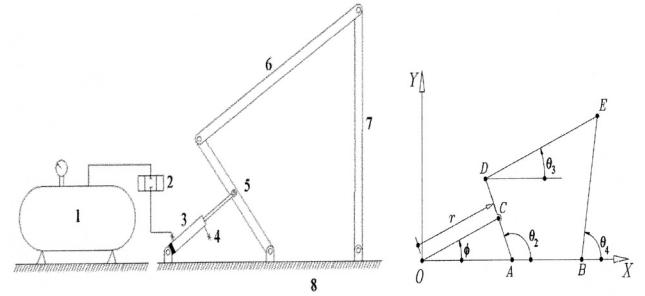


Figure 3. Complete system. (a) Schematic diagram including tank (1), directional control valve (2), pneumatic cylinder (3), braking device (4), and four bar linkage (5, 6, 7 and 8), (b) Kinematic layout of the actuated four bar linkage.

$$\theta_3 = 2 \arctan \left(\frac{-C \pm \sqrt{C^2 + D^2 - E^2}}{E - D} \right) \quad (35)$$

$$\theta_4 = 2 \arctan \left(\frac{-F \pm \sqrt{F^2 + G^2 - H^2}}{H - G} \right) \quad (36)$$

where: $d \equiv AD$, $s \equiv DE$, $h \equiv AB$, $l \equiv BE$,
 $C \equiv 2sd \sin \theta_2$, $D \equiv 2sd \cos \theta_2 - 2sh$, $E \equiv d^2 + s^2 + h^2 - l^2 - 2hd \cos \theta_2$,
 $F \equiv 2hd \sin \theta_2$, $G \equiv 2hd \cos \theta_2 - 2h$, $H \equiv s^2 - d^2 - l^2 - h^2 + 2hd \cos \theta_2$

Similarly the joint velocity vector $\dot{q} = (\dot{r}, \dot{\phi}, \dot{\theta}_2, \dot{\theta}_3, \dot{\theta}_4)^T$ and the joint acceleration vector $\ddot{q} = (\ddot{r}, \ddot{\phi}, \ddot{\theta}_2, \ddot{\theta}_3, \ddot{\theta}_4)^T$ are defined as function of the time derivatives of the joint variables. Thus, given the input velocity \dot{r} and the input acceleration \ddot{r} a closed-form solution for the remaining joint velocities and joint accelerations are defined by the following equations in addition to equations (4), (5), (6) and (7):

$$\dot{\theta}_3 = \frac{\dot{\theta}_2 d \sin(\theta_2 - \theta_4)}{s \sin(\theta_4 - \theta_3)} \quad (37)$$

$$\dot{\theta}_4 = \frac{\dot{\theta}_2 d \sin(\theta_2 - \theta_3)}{l \sin(\theta_4 - \theta_3)} \quad (38)$$

$$\ddot{\theta}_3 = \frac{\dot{\theta}_2^2 d \cos(\theta_2 - \theta_4) + \ddot{\theta}_2 d \sin(\theta_2 - \theta_4) + s \dot{\theta}_3^2 \cos(\theta_3 - \theta_4) - l \dot{\theta}_4}{s \sin(\theta_4 - \theta_3)} \quad (39)$$

$$\ddot{\theta}_4 = \frac{\dot{\theta}_2^2 d \cos(\theta_2 - \theta_3) + \ddot{\theta}_2 d \sin(\theta_2 - \theta_3) - l \dot{\theta}_4^2 \cos(\theta_4 - \theta_3) - s \dot{\theta}_3}{l \sin(\theta_4 - \theta_3)} \quad (40)$$

The solution of the acceleration equations, given by equations (6), (7), (39) and (40), completes the joint kinematics analysis.

Point kinematics

For the purposes of this paper, *point kinematics* means to obtain vector expressions for the position, velocity and acceleration of those linkage points which are of interest for the analyst. Moreover, they will be formulated in terms of the joint motion variables q, \dot{q}, \ddot{q} and the geometric properties of the linkage. It is obvious that the mass center points of the moving links, G_2, G_3 , and G_4 , are points of interest in the dynamic analysis. Thus, referring to Fig. 4, their corresponding position, velocity and acceleration are given by the following vectors:

$$\mathbf{r}_{G2} = r_{21} \cos(\theta_2 + \gamma_2) \mathbf{i} + r_{21} \sin(\theta_2 + \gamma_2) \mathbf{j} \quad (41)$$

$$\mathbf{r}_{G3} = [d \cos \theta_2 + r_{32} \cos(\theta_3 + \gamma_3)] \mathbf{i} + [d \sin \theta_2 + r_{32} \sin(\theta_3 + \gamma_3)] \mathbf{j} \quad (42)$$

$$\mathbf{r}_{G4} = [h + r_{44} \cos(\theta_4 + \gamma_4)] \mathbf{i} + r_{44} \sin(\theta_4 + \gamma_4) \mathbf{j} \quad (43)$$

$$\mathbf{v}_{G2} = -r_{21} \dot{\theta}_2 \sin(\theta_2 + \gamma_2) \mathbf{i} + r_{21} \dot{\theta}_2 \cos(\theta_2 + \gamma_2) \mathbf{j} \quad (44)$$

$$\mathbf{v}_{G3} = -[\dot{\theta}_2 d \sin \theta_2 + r_{32} \dot{\theta}_3 \sin(\theta_3 + \gamma_3)] \mathbf{i} + [\dot{\theta}_2 d \cos \theta_2 + r_{32} \dot{\theta}_3 \cos(\theta_3 + \gamma_3)] \mathbf{j} \quad (45)$$

$$\mathbf{v}_{G4} = -r_{44} \dot{\theta}_4 \sin(\theta_4 + \gamma_4) \mathbf{i} + r_{44} \dot{\theta}_4 \cos(\theta_4 + \gamma_4) \mathbf{j} \quad (46)$$

$$\mathbf{a}_{G2} = -[r_{21} \dot{\theta}_2^2 \cos(\theta_2 + \gamma_2) + r_{21} \ddot{\theta}_2 \sin(\theta_2 + \gamma_2)] \mathbf{i} - [r_{21} \dot{\theta}_2^2 \sin(\theta_2 + \gamma_2) + r_{21} \ddot{\theta}_2 \cos(\theta_2 + \gamma_2)] \mathbf{j} \quad (47)$$

$$\mathbf{a}_{G3} = -[\ddot{\theta}_2 d \cos \theta_2 + \ddot{\theta}_2 d \sin \theta_2 + r_{32} \dot{\theta}_3^2 \cos(\theta_3 + \gamma_3) + r_{32} \ddot{\theta}_3 \sin(\theta_3 + \gamma_3)] \mathbf{i} + [\ddot{\theta}_2 d \cos \theta_2 + r_{32} \dot{\theta}_3 \cos(\theta_3 + \gamma_3) - \ddot{\theta}_2 d \sin \theta_2 - r_{32} \dot{\theta}_3 \sin(\theta_3 + \gamma_3)] \mathbf{j} \quad (48)$$

$$\mathbf{a}_{G4} = -[r_{44} \dot{\theta}_4^2 \cos(\theta_4 + \gamma_4) + r_{44} \ddot{\theta}_4 \sin(\theta_4 + \gamma_4)] \mathbf{i} - [r_{44} \dot{\theta}_4^2 \sin(\theta_4 + \gamma_4) + r_{44} \ddot{\theta}_4 \cos(\theta_4 + \gamma_4)] \mathbf{j} \quad (49)$$

being \mathbf{i} and \mathbf{j} unit vectors along the X and Y axis, respectively (see also Fig. 3) and the involved geometric parameters were defined as follows:

$$r_{21} \equiv AG_2, r_{22} \equiv DG_2, r_{32} \equiv DG_3, r_{33} \equiv EG_3, r_{43} \equiv EG_4 \text{ and } r_{44} \equiv BG_4$$

Thus, expressions (47), (48), and (49) will be used presently in the equations of motion, as is shown in the next section.

Dynamic analysis

Before starting with the formulation of the equations of motion, it is necessary to make a free-body diagram for each one of the links of the four bar linkage, as it is now shown in Fig. 4. Then, according to Newton's Second Law applied for each free-body diagram, the following matrix equation may be written:

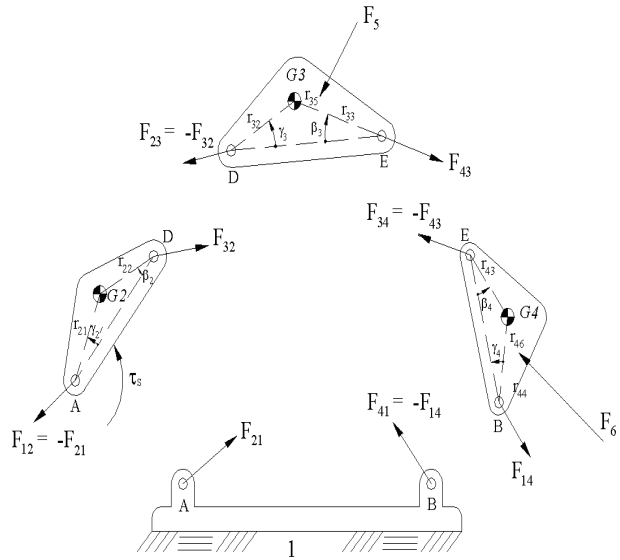


Figure 4. Free body diagram of each link of the four bar linkage.

$$\mathbf{D} \mathbf{a} = \mathbf{b} \quad (50)$$

where:

$$\mathbf{D} \equiv \begin{bmatrix} -1 & 0 & 1 & 0 & 0 & 0 & 0 & 0 & 0 & 0 \\ 0 & -1 & 0 & 1 & 0 & 0 & 0 & 0 & 0 & 0 \\ r_{21y} & -r_{21x} & -r_{22y} & r_{22x} & 0 & 0 & 0 & 0 & 0 & 1 \\ 0 & 0 & -1 & 0 & 1 & 0 & 0 & 0 & 0 & 0 \\ 0 & 0 & 0 & -1 & 0 & 1 & 0 & 0 & 0 & 0 \\ 0 & 0 & r_{32y} & -r_{32x} & -r_{33y} & r_{33x} & 0 & 0 & 0 & 0 \\ 0 & 0 & 0 & 0 & -1 & 0 & 1 & 0 & 0 & 0 \\ 0 & 0 & 0 & 0 & 0 & -1 & 0 & 1 & 0 & 0 \\ 0 & 0 & 0 & 0 & r_{43y} & -r_{43x} & -r_{44y} & r_{44x} & 0 & 0 \end{bmatrix}$$

$$\mathbf{a} \equiv \begin{bmatrix} F_{21x} \\ F_{21y} \\ F_{32x} \\ F_{32y} \\ F_{43x} \\ F_{43y} \\ F_{14x} \\ F_{14y} \\ \tau_s \end{bmatrix} \quad \text{and} \quad \mathbf{b} \equiv \begin{bmatrix} m_{b2} a_{G2x} \\ m_{b2} a_{G2y} \\ I_2 \ddot{\theta}_2 \\ m_{b3} a_{G3x} - F_{5x} \\ m_{b3} a_{G3y} - F_{5y} \\ I_3 \ddot{\theta}_3 + r_{35y} F_{5x} - r_{35x} F_{5y} \\ m_{b4} a_{G4x} - F_{6x} \\ m_{b4} a_{G4y} - F_{6y} \\ I_4 \ddot{\theta}_4 + r_{46y} F_{6x} - r_{46x} F_{6y} \end{bmatrix}$$

where m_{b2}, m_{b3} and m_{b4} represent the mass of links 2, 3 and 4 respectively, and I_2, I_3 and I_4 the mass moment of inertia of links 2, 3 and 4 respectively, and:

$$\begin{aligned}
r_{21y} &\equiv r_{21} \sin(\theta_2 + \gamma_2), & r_{21x} &\equiv r_{21} \cos(\theta_2 + \gamma_2) \\
r_{22y} &\equiv r_{22} \sin(\theta_2 + \beta_2), & r_{22x} &\equiv r_{22} \cos(\theta_2 + \beta_2) \\
r_{32y} &\equiv r_{32} \sin(\theta_3 + \gamma_3), & r_{32x} &\equiv r_{32} \cos(\theta_3 + \gamma_3) \\
r_{33y} &\equiv r_{33} \sin(\theta_3 + \beta_3), & r_{33x} &\equiv r_{33} \cos(\theta_3 + \beta_3) \\
r_{43y} &\equiv r_{43} \sin(\theta_4 + \gamma_4), & r_{43x} &\equiv r_{43} \cos(\theta_4 + \gamma_4) \\
r_{44y} &\equiv r_{44} \sin(\theta_4 + \beta_4), & r_{44x} &\equiv r_{44} \cos(\theta_4 + \beta_4)
\end{aligned}$$

Solution of equation (50) may be found numerically or analytically. An algebraic solution was obtained by Pérez-Meneses (2003). In particular, the force on the cylinder may be obtained in terms of torque τ_s by the next equation, where F_1 is the force applied to the linkage by the pneumatic piston:

$$F_1 = \frac{\tau_s}{r \cos(\phi + \delta_2) \sin \phi + \sin(\phi + \delta_2)(L - r \cos \phi)} \quad (51)$$

τ_s is the resultant torque produced by all the external forces acting on the four bar linkage. Thus, force F_1 will be used into the thermodynamic equations by incorporating the work done by this force on the system.

Thermodynamic equations

In order to incorporate the influence of the air properties into the whole model, a similar procedure to that developed for a pivoted link is follow, then applying the First Law of Thermodynamics and the basic equation for ideal gases, the following modeling equation is obtained:

$$\begin{aligned}
&\left[\frac{2Cv(V_0 + A(r - r_0))}{AR} \right] \ddot{r} - \left[r - \frac{2Cv(V_0 + A(r - r_0))}{AR} \right] r \dot{\phi}^2 + \left[\dot{r} + \frac{2Cv(V_0 + A(r - r_0))}{m_p AR} \right] \dot{r} + \\
&+ \left[\left(\frac{V_0 + A(r - r_0)}{AR} \right) (P_A A_A + F_F + F_{Fd} + F_{Fs}) - m_l T_1 \right] \frac{2Cv}{m_p} - \frac{2Cp T_0}{m_p} (m_2 - m_1) + \\
&+ \left[(F_F + F_{Fd} + F_{Fs})(r - r_0) + \int P_A A_A dr + \int C_F dr \right] \frac{2}{m_p} - \frac{2}{m_p} Q + 2(r - r_0) r \dot{\phi} + \\
&+ \left[\frac{2Cv(V_0 + A(r - r_0))}{m_p AR} \right] \frac{2(r - r_0)}{m_p} \left[\frac{\tau_s}{r \cos(\phi + \delta_2) \sin \phi + \sin(\phi + \delta_2)(L - r \cos \phi)} \right] = 0 \quad (52)
\end{aligned}$$

In order to incorporate friction forces into the model, the following procedure is proposed:

When $\dot{r} \neq 0$ then $F_F = F_D \operatorname{sign}(\dot{r})$

When $\dot{r} = 0$

if $(P_A - P_A A_A) \leq F$ then $F_F = F_S$
if $(P_A - P_A A_A) \leq -F$ then $F_F = -F_S$
if $|P_A - P_A A_A| < F_S$ then $F_F = P_A - P_A A_A$

where F_F is the friction force, F_D is the dynamic friction force, F_S is the static friction force, P is the pressure on the high-pressure side of the piston, A is the area of the inlet side of the piston, P_A is the pressure on the low-pressure side of the piston, and A_A is the area on the outlet side of the piston.

Simulation Procedure

The mathematical model was run using the experimental parameters as defined in Table 2.

A computer program based into the flow chart presented in Fig. 5 was designed in order to solve the mathematical model. Moreover, Runge Kutta fourth order method, Korn A. G., Korn T. M. (1968), was used to integrate equations (6) and (52), using a time increment of 0.001s as the integration parameter.

Table 1. Characteristic of elements for the basic model

Element	Characteristic	Value or Range
1. Pressurized air tank	Volume, m ³	0.05
	Pressure, kPa	200 to 400
2. On-Off Valve	Nominal pressure, kPa	-95 to 1000
	Nominal flow, l/min	700
3. Filter	Solid size, μm	40
	Nominal temperature, °K	263 to 333
4. High pressure line	Inside diameter, m	0.0065
	Length, m	1.26
5. Pressure gage	Maximum pressure, kPa	0 to 1200
6. Pneumatic cylinder	Piston stroke, m	0.1
	Piston area, m ²	0.00196
	Braking stroke, m	0.024
	Initial length of cylinder, m	0.364
	Outlet area, m ²	0.000176
7. Exhaust valve	Coefficient value	0.1 to 0.7
8. Pivoted link	Parameter L, m	0.464
	Parameter p, m	0.223
	Total length d, m	0.446
	Mass, kg	1.2
	Additional mass, kg	4.3 to 8.6
	Moment of inertia for each mass, kg·m ²	0.07956 to 0.5702
9. Signal amplifier	Transducer sense, pC/ms ²	0.1 to 11
	mV/Unit out, mV/mms ⁻²	0.1 to 1000
	Lower freq limit, Hz	0.01 to 10
	Upper freq limit, kHz	0.1 to 100
10. PC Computer	Maximum input voltage in card data, V	±5

EXPERIMENTAL ANALYSIS

Basic Model.

The experimental apparatus used to monitor the acceleration of a point on the pivoted link is shown in Fig. 6. This includes components with characteristics as described in Table 1. Most of those characteristics were obtained from the manufacturer. The pivoted link was fabricated in the university work shop and its characteristics obtained from geometrical dimensions. A special experiment was run to adjust the coefficient value of the exhaust valve which was obtained experimentally for each one of several positions of the adjusting bolt. Fig. 7 shows the conceptual diagram of the experiment for such a purpose. The experiment was run for each

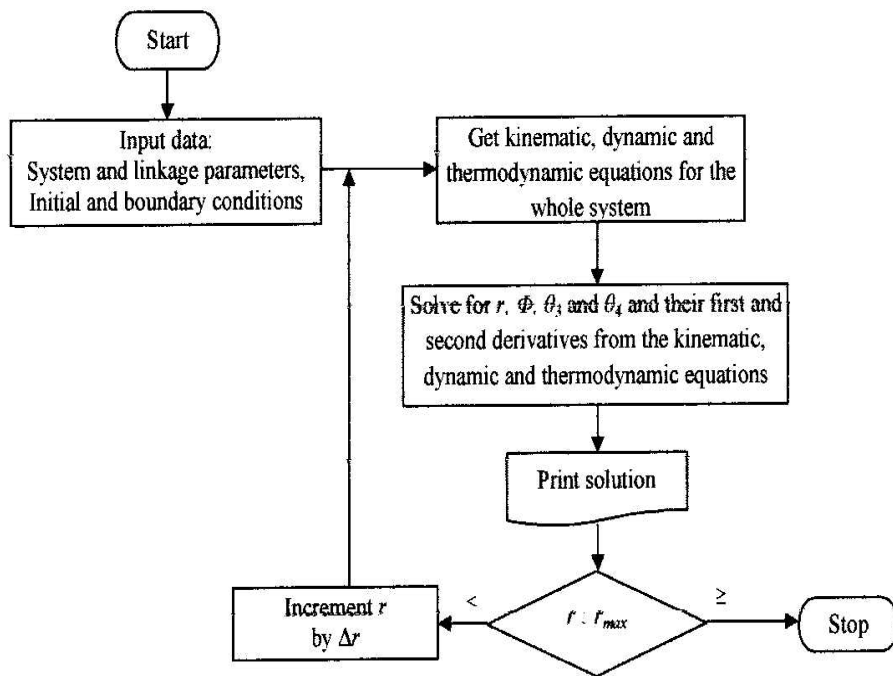


Figure 5. Flow diagram used for the numerical solution of the whole system.

position of the adjusting bolt recording the experimental response in the computer. Values of the coefficient were adjusted until the theoretical response became close to the experimental one, for a particular set of conditions. Theoretical response for this case was obtained from the following equation, Aguilera-Gomez, E. and Lara-Lopez.

$$\left[\frac{2C_v(V_0 + Ar)}{AR} \right] \ddot{r} + \dot{r} \left[\dot{r} + \frac{2C_v(V_0 + Ar)C}{m_p AR} \right] + \frac{2}{m_p} \left(\int F dr + \int P_A A_A dr + \int C \dot{r}^2 dr \right) +$$

$$+ \frac{2C_v}{m_p} \left[\left(\frac{V_0}{AR} \right) (P_A A_A + F_F + F) - m_1 T_1 \right] - \frac{2C_p T_0}{m_p} (m_2 - m_1) +$$

$$+ r \left\{ \left(\frac{2}{m_p} \right) \left[\left(\frac{C_v}{R} \right) (P_A A_A + F_F + F) + F_F \right] \right\} - \frac{2Q}{m_p} = 0 \quad (53)$$

Comparison of theoretical and experimental responses

Figure 8 shows the comparison of the theoretical and experimental responses, for the coefficient of exhaust valve and end cushion device. The coefficient previously determined was confirmed for several conditions varying the lifting weights and air pressure.

Once the values for all variables of table 1 were obtained, the mathematical model and experimental apparatus for the pivoted link were run and compared as shown in Fig. 9.

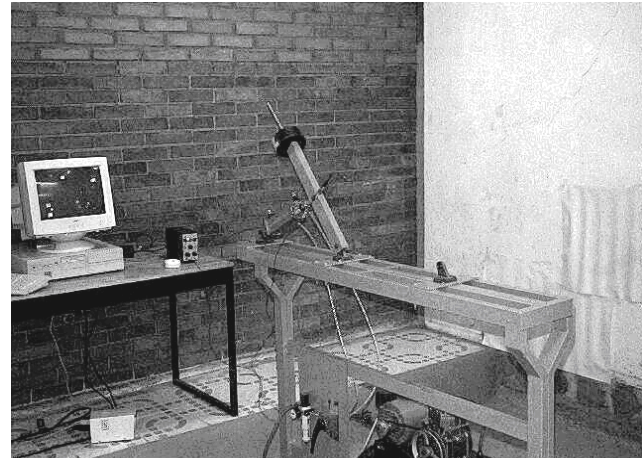


Figure 6. Experimental apparatus used to monitor the acceleration of the pivoted link.

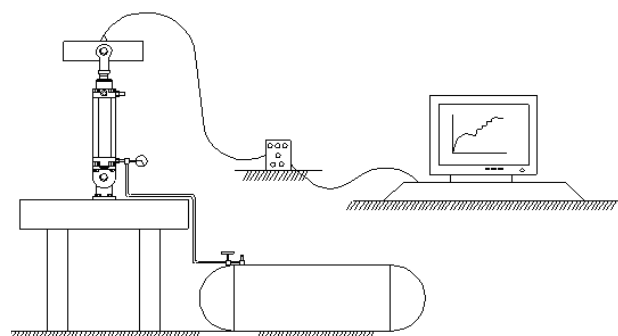


Figure 7. Conceptual diagram of the experiment for evaluation of the exhaust valve coefficient.

Table 2. Characteristic of elements for the four bar linkage

Element	Characteristic	Value or Range
1. Pressurized air tank	Volume, m^3	0.05
	Pressure, kPa	200 - 400
2. Atmospheric conditions	Temperature, $^{\circ}\text{K}$	293.15
	Pressure, kPa	81.60
3. Pneumatic cylinder	Piston stroke, m	0.1
	Piston area, m^2	0.00196
	Outlet area, m^2	0.000176
	Braking stroke, m	0.024
	Initial angular position, radians	0.4899
	Initial length, m	0.364
4. Exhaust valve	Coefficient	0.1
5. Linkage	Length of link 1, m	0.40
	Length of link 2, m	0.50
	Length of link 3, m	0.85
	Length of link 4, m	0.80
	Mass of link 2, kg	2.50
	Mass of link 3, kg	3.20
	Mass of link 4, kg	4.50
	Centroidal mass moment of inertia of link 2, $\text{kg}\cdot\text{m}^2$	0.0521
	Centroidal mass moment of inertia of link 3, $\text{kg}\cdot\text{m}^2$	0.1926
	Centroidal mass moment of inertia of link 4, $\text{kg}\cdot\text{m}^2$	0.2400

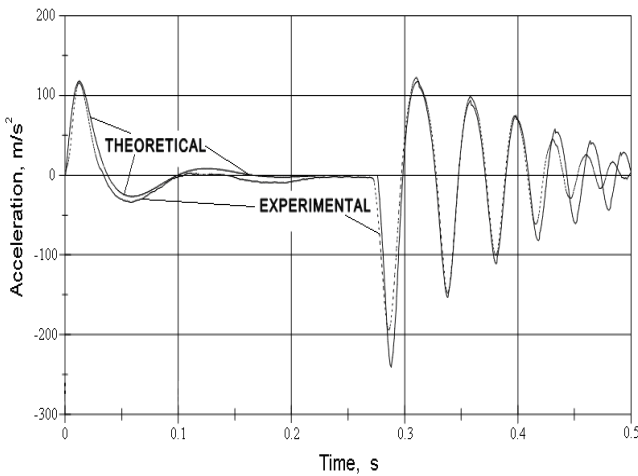


Figure 8. Numerical and experimental response of the system.
The response is obtained for the cylinder in a vertical position and the exhaust valve coefficient adjusted for theoretical response.

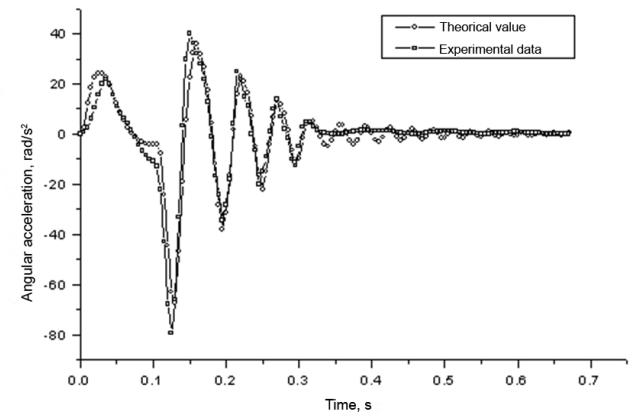


Figure 9. Comparison of theoretical and experimental angular acceleration of the pivoted link.

Figures 10 and 11 were obtained by numerical integration from the data corresponding to Fig. 9.

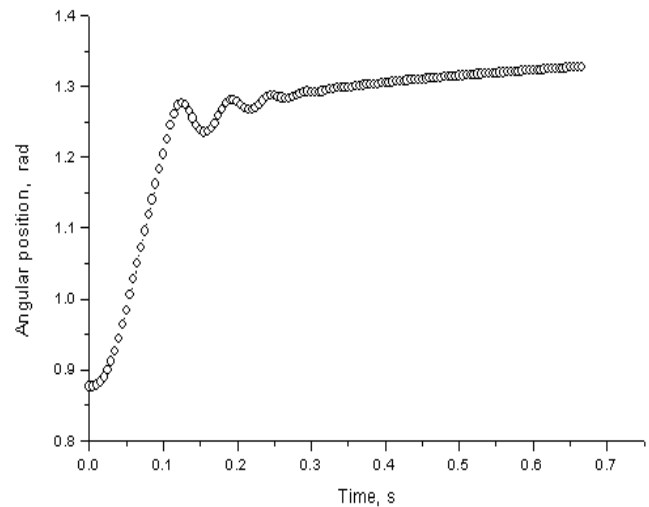


Figure 10. Numerical result for the angular position of the pivoted link.

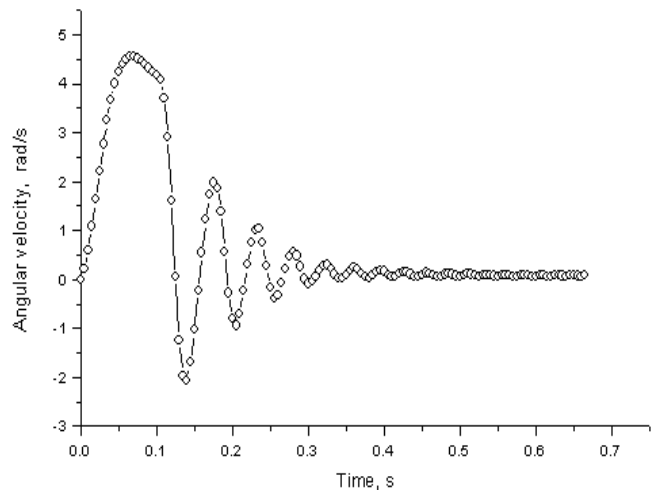


Figure 11. Numerical result for the angular velocity of the pivoted link.

Figures 12, 13 and 14 show the effect on the response of the system due to changes on the dimensions linkage. Fig. 12 shows the effect of length of link, p , on the total extending time, maintaining the other lengths constant. Fig. 13 shows the effect of the length link L on the total extending time, and finally Fig. 14 shows the effect of the position of the link mass center r_{21} on the total extending time.

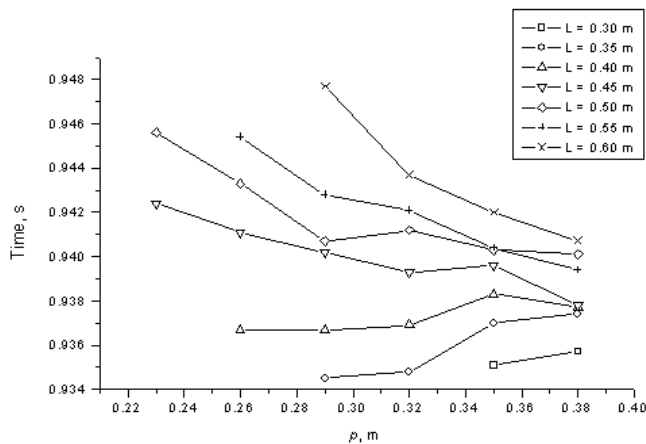


Figure 12. Effect of parameter p on the total extending time, for different values of L .

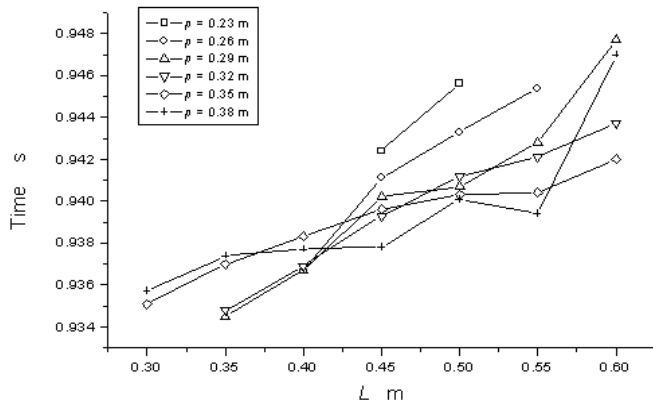


Figure 13. Effect of parameter L on the total extending time, for different values of p .

The difference between the theoretical response and the experimental one is about 1.5% for minimum acceleration and 3.2% for maximum acceleration. These differences may be due to an error in the transducer performance caused by changes in the temperature, calibration or humidity in the testing room.

In addition, the model offers the possibility for sensitivity analysis varying a parameter of the system. An example of this feature is shown in Fig. 15 where the pressure of the tank is varied and the effect on the period of time for full extension of the cylinder can be seen. Another interesting effect can be seen in Fig. 16, where the influence of the volume of the air tank on the period for full extension is plotted for a constant initial pressure.

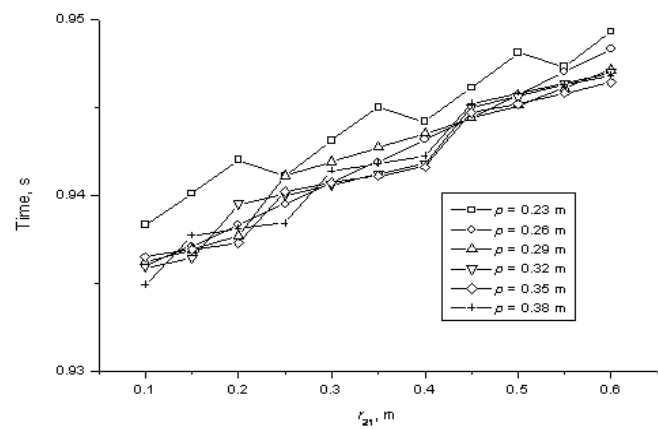


Figure 14. Effect of the position of the center of mass of the link r_{21} , on the total extending time.

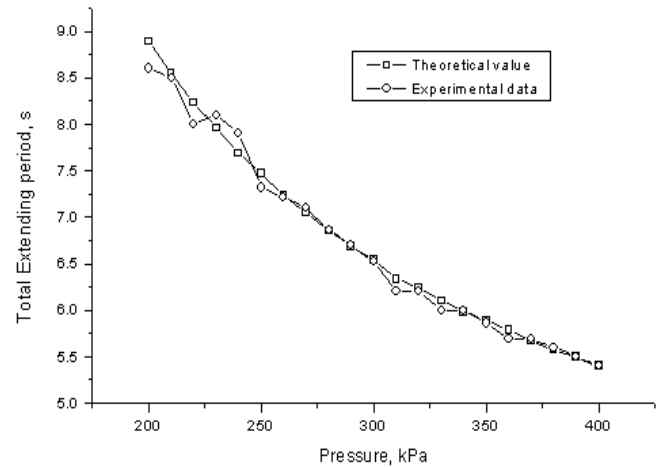


Figure 15. Effect of the pressure tank on the total extending time.

Four bar linkage.

A mechanical system, similar to the one shown in Fig. 3, was designed and constructed. Such a system is shown in Fig. 17. Moreover, the external force on the output link was provided by a compression spring which is pivoted around the two extreme points. Finally, the main characteristics of the involved components are defined in Table 2.

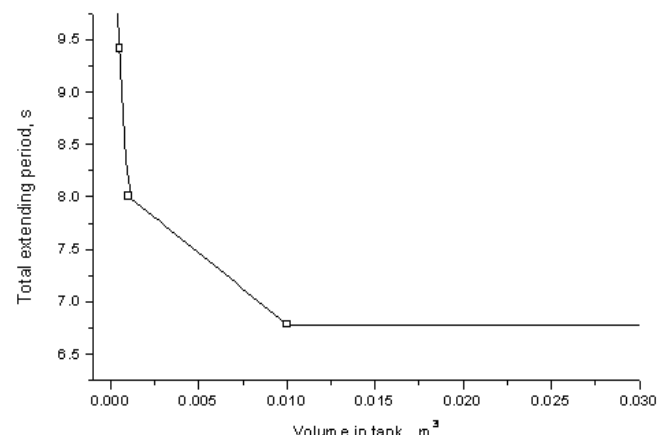


Figure 16. Effect of tank volume on the total extending time for an initial pressure of 290 kPa.



Figure 17. Experimental apparatus used to verify the whole model.

An acceleration sensor was mounted on the output link to obtain the tangential acceleration. Thus, signal from the sensor was amplified before processing the data into a PC computer Data Acquisition system. By means of computer software, plots of the acceleration as function of time were obtained. Additionally, in order to assure the confidence on the experimental results, the experiment was conducted several times. Then, the experimental response was recorded each 0.001 seconds. Figure 18 shows the response obtained in one of the experimental runs.

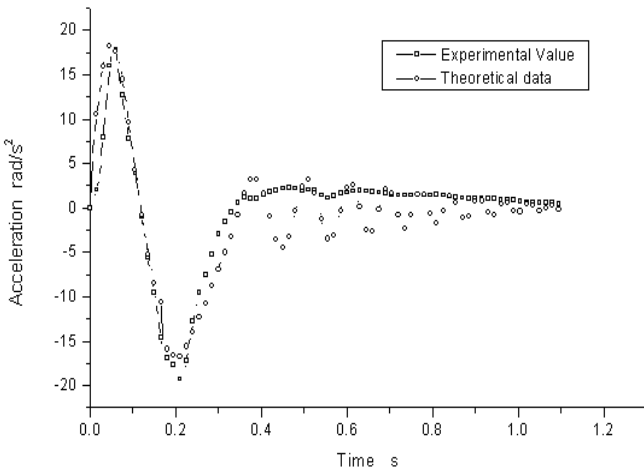


Figure 18. Theoretical and experimental response of system.

Comparison of theoretical and experimental responses

Based on Fig. 18, it can be concluded that both responses, experimental and theoretical, have similar shape. However, it can be noted that the experimental response is less sensitive to oscillations probably due to dry friction on articulated joints. Moreover, the velocity and the position of the output link may be obtained by numerical integration of the theoretical response, as shown in Figs. 19 and 20. Also, the effect of any parameter of the system on the response may be predicted with the aid of the mathematical model. For instance, Fig. 21 shows the effect of tank pressure on the total extending time. Other parameters such as tank volume, air temperature, and linkage weight or linkage size may be modified in order to investigate the effect of such variables on the response of the system.

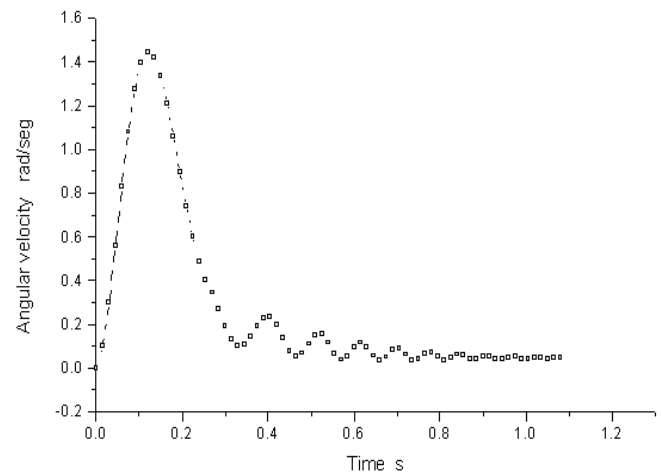


Figure 19. Numerical result for the angular velocity of the output link.

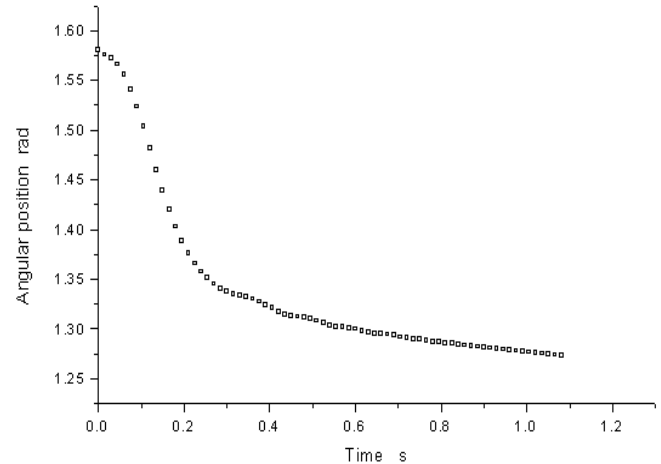


Figure 20. Numerical result for the angular position of the output link

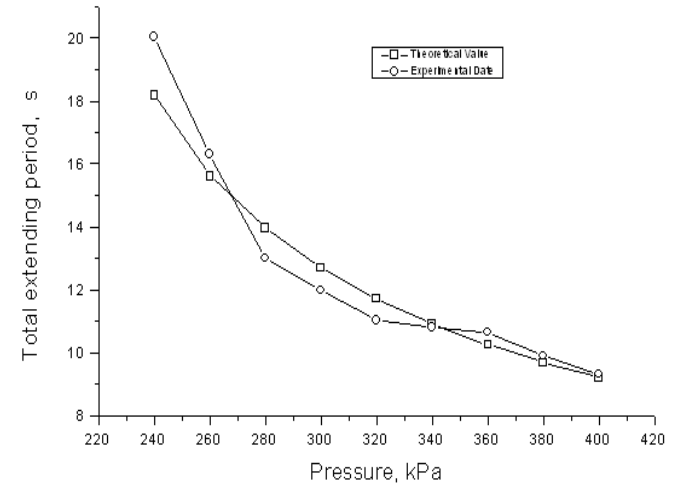


Figure 21. Effect of the pressure of tank on the total extending period of piston.

CONCLUSIONS

The mathematical model based on fundamental principles of mechanics and thermodynamics allows prediction of dynamic response of the pivoted link and four bar linkages.

The shape and absolute values for the theoretical response are in good agreement with the experimental response for both cases.

Influence of system parameters may be analyzed by the proposed mathematical model, including size of components such as tank volume or dimensions of piston.

The problems discussed are highly nonlinear. However some simplifying assumptions could be made when the tank is large enough, such as considering pressure as a constant and heat exchange negligible.

The theoretical model incorporates two nonlinear ordinary differential equations. Previously published models are more complex. The incorporation of rigid body dynamic principles contributed to simplify the mathematical model.

The theoretical model may be used as a base to aid analysis, design and optimization of systems incorporating four bar linkages pneumatically driven.

Acknowledgments

Authors have a debt of gratitude with the school of Mechanical and Electrical Engineering of the University of Guanajuato at Salamanca, Mexico, for all support given to this research project. Thanks to scholarships from the National Council for Science and Technology of Mexico and from the Council for Science and Technology of the State of Guanajuato, granted to the second author, it was possible to complete the research project.

REFERENCES

Aguilera-Gomez, E. and Lara-Lopez, A. *Dynamics of a pneumatic system: modeling, simulation and experiments. International Journal of Robotics and Automation*, 1999, **14**(1), 39-43.

Anderson B. W. *The Analysis and Design of Pneumatic Systems*, 2001, Krieger publishing Company, Malabar Florida, USA.

Brobrow, J. E. and Jabbari, F. *Adaptive pneumatic force actuation and position control. Transactions of the ASME, Journal of Dynamic Systems, Measurement and Control*, 1991, **113**, 267-272.

Kawakami, Y., Akao, J., and Kawai, S. *Some considerations on the dynamic characteristics of pneumatic cylinders. Journal of Fluid Control Including Fluidics*, 1988, **20**, 22 - 26.

Kiczkowiak, T. *Simplified Mathematical model of the pneumatic high speed machine drive. Mechanisms and Machine Theory*, 1995, **30**(1), 101-107.

Korn A. G., Korn T. M. *Mathematical Handbook for Scientists and Engineers*, Second Edition, 1968, McGraw-Hill Book Company, 777-785.

Shigley J. E. and Uicker J. J. Jr. *Theory of machines and mechanisms*, Second Edition, 1995, McGraw-Hill Book Company.

Skreiner, M. and Barkan, P. *On a model of a pneumatically actuated mechanical system. Transactions of the ASME, Journal of Engineering for Industry*, 1971, **93**, 211-220.

Perez-Meneses, J. *Dynamic analysis of pneumatically driven mechanisms, Doctoral Dissertation. Department of Mechanical Engineering, University of Guanajuato*, 2003.

Tang, J. and Walker, G. *Variable structure control of a pneumatic actuator. Transactions of the ASME, Journal of Dynamic Systems, Measurement and Control*, 1995, **117**, 88-93.